PCCP

View Online
Dynamic Article Links

Cite this: *Phys. Chem. Chem. Phys.*, 2011, **13**, 17378–17383

www.rsc.org/pccp

PAPER

Slow photoelectron velocity-map imaging spectroscopy of the phenoxide and thiophenoxide anions

Jongjin B. Kim,[a] Tara I. Yacovitch,[a] Christian Hock[a] and Daniel M. Neumark*[ab]

Received 6th July 2011, Accepted 8th August 2011
DOI: 10.1039/c1cp22211b

High resolution anion photodetachment spectra of the phenoxide and thiophenoxide anions were obtained with slow electron velocity-map imaging. The spectra show transitions to the $\tilde{X}^2B_1$ neutral states of both species and to the $\tilde{A}^2B_2$ state of the thiophenoxy radical. Comparison of the spectra with Franck-Condon simulations allows several gas-phase vibrations to be assigned. The adiabatic electron affinities are determined to be 2.2538(8) eV and 2.3542(6) eV for phenoxy and thiophenoxy, respectively. The term energy of the $\tilde{A}^2B_2$ state of thiophenoxy is found to be 0.3719(9) eV, higher than the values reported in photodissociation experiments of thiophenol.

Introduction

The phenoxy radical has been extensively studied theoretically and spectroscopically over many years. It is an important intermediate in the combustion of aromatic compounds.[1,2] Furthermore, as itself or as the functional component of the amino acid tyrosine, it participates in many aspects of biology, ranging from redox chemistry to photosynthesis.[3,4] Thiophenoxy, the sulfur analogue, has seen considerable use as a capping ligand for CdS nanoparticles,[5,6] but until recently little spectroscopic work had been performed on it. In this paper, we present high-resolution photodetachment spectra of the phenoxide and thiophenoxide anions that probe the energetics and vibrations of the corresponding neutral radicals.

Phenoxy has been investigated by many different methods. The nature of its unpaired electron has been studied by electron spin resonance spectroscopy.[7–9] Vibrational frequencies were determined in solution by resonance Raman spectroscopy,[10,11] in rare-gas matrices by IR spectroscopy,[12] and in the gas phase by photoelectron (PE) spectroscopy of the phenoxide anion.[13] Electronic transitions have also been studied by absorption in the gas phase, solution, and rare-gas matrices.[14,15] Recently, cavity-ringdown spectroscopy was used to determine the rovibronic bands of the optically-forbidden $\tilde{A}^2B_2 \leftarrow \tilde{X}^2B_1$ transition.[16] The electron affinities (EAs) of phenoxy and thiophenoxy were obtained from anion photodetachment spectroscopy.[17] An improved EA for phenoxy was determined by the phenoxide photoelectron spectrum.[13] Some vibrational frequencies of thiophenoxy were determined in solution by resonance Raman spectroscopy[18] and in gas phase by laser-induced fluorescence.[19] Vibrational frequencies have been calculated for the phenoxy and thiophenoxy radicals in some of these experimental studies[12,13,18] and in several purely theoretical works.[20–26]

The phenoxy and thiophenoxy radicals are also of interest as the products of phenol[27–30] and thiophenol[25,31] photodissociation. The photochemistry of phenol has long been of interest as a model for biological chromophores. Experimental and theoretical work discussed by Sobolewski *et al.*[32] has emphasized the importance of conical intersections in the photodissociation of phenol and other aromatic species that lose an H atom upon electronic excitation. For example, in phenol, the initially excited $^1\pi\pi^*$ S_1 state is crossed by the repulsive $^1\pi\sigma^*$ S_2 state. Moving further along the O–H coordinate, the S_2 curve crosses the S_0 curve, forming a conical intersection, with the CCOH rotor believed to be the coupling mode. The S_0 curve correlates diabatically to the phenoxy $\tilde{A}^2B_2$ state, which has the unpaired electron located in an in-plane p orbital on the oxygen atom. The S_2 curve correlates to the $\tilde{X}^2B_1$ state, with the unpaired electron delocalized in the out-of-plane π-bonding network.

Ashfold and co-workers have studied the photodissociation of phenol with H-atom Rydberg tagging, yielding a high resolution photofragment translational energy distribution for the H-atom loss channel.[28,29] They observed production of the phenoxy $\tilde{X}^2B_1$ channel with vibrational resolution, but did not observe the $\tilde{A}^2B_2$ state, which lies 0.952 eV above the $\tilde{X}^2B_1$ state.[16] The $\tilde{A}^2B_2 \leftarrow \tilde{X}^2B_1$ energy separation is considerably smaller for thiophenoxy. Photodissociation experiments on thiophenol by Lim *et al.*[26,33,34] using ion imaging and by Devine *et al.*[25] using Rydberg tagging yielded bimodal translational energy distributions, indicating that both thiophenoxy states were produced. Based on these distributions, they reported Ã–$\tilde{X}$ term values of 0.32(2) eV and 0.347(5) eV, respectively.

Anion PE spectroscopy provides an alternative technique to probe the spectroscopy and energetics of the phenoxy and

[a] *Department of Chemistry, University of California, Berkeley, California 94720, USA. E-mail: dneumark@berkeley.edu*
[b] *Chemical Sciences Division, Lawrence Berkeley National Laboratory, Berkeley, California 94720, USA*

thiophenoxy radicals, as demonstrated by the PE spectrum of phenoxide reported by Gunion *et al.*[13] In this paper, we report higher-resolution PE spectra of the phenoxide and thiophenoxide anions with slow electron velocity-map imaging (SEVI).[35] Vibrationally-resolved transitions to the $\tilde{X}^2B_1$ state of each radical species are obtained, and photodetachment to the $\tilde{A}^2B_2$ excited state of the thiophenoxy radical, a fully allowed transition in photoelectron spectroscopy, is also well-resolved. Assignments of the electronic and vibrational transitions are supported by electronic structure calculations and Franck-Condon (FC) simulations. We obtain accurate electron affinities for both radicals and a term energy for the $\tilde{A}^2B_2$ state of thiophenoxy that is somewhat higher than previously reported values.[25,26]

Experiment

The SEVI apparatus used to obtain high-resolution PE spectra of phenoxide and thiophenoxide has been previously described in detail.[35,36] Briefly, mass-selected anions were photodetached using a tunable dye laser. The ejected photoelectrons were collected by velocity-map imaging (VMI)[37] using low extraction voltages. Slow electrons were imaged and a high-resolution PE spectrum was obtained over a narrow energy window. Spectra were taken at several wavelengths to obtain high resolution over a wider range.

Phenoxide anions were produced from a mixture of ~0.1% benzene and ~0.1% N_2O in argon, while thiophenoxide ions were produced from ~0.1% thiophenol in argon. At 300 psi stagnation pressure, the gas mixtures were expanded into vacuum with an Even-Lavie pulsed valve.[38] Anions were created from this expansion using a dc discharge grid[39] and injected into a Wiley-McLaren time-of-flight spectrometer,[40] which directed the anions to the detachment region. Ions of the desired mass were intersected and photodetached between the repeller and extraction plates of the VMI stack by the focused output of a Nd:YAG-pumped tunable dye laser. The resulting photoelectron cloud was coaxially extracted down a 50 cm flight tube to an imaging detector, comprising a pair of time-gated chevron-stacked microchannel plates coupled to a phosphor screen, as is standard for photoelectron imaging experiments.[41] The image on the phosphor was collected with a 1024 × 1024 charge-coupled device (CCD) camera and recorded on a computer. Images were summed, quadrant-symmetrized, smoothed, and inverse-Abel transformed[42] to recover the 3D distribution from the 2D projection of the photoelectron cloud. PE spectra were obtained by angular integration of the transformed images. Spectra are reported in electron binding energy (eBE), defined as the difference between the photodetachment energy and the electron kinetic energy (eKE).

The apparatus was calibrated to high-resolution literature values on the photodetachment transitions of the sulfide anion.[43,44] With the −350 V VMI repeller voltage used in this study, a Gaussian width (2σ) of 4.7 cm^{-1} was obtained for a sulfide peak with an eKE of 53.6 cm^{-1}. In the SEVI experiment, the resolution is given by the pixel width for each transition on the image, which is approximately constant. Since the radius is proportional to the electron velocity in a VMI image, the resolution in eKE is greater at smaller radius, and the energy resolution is greatest near threshold. To obtain a complete high resolution spectrum, several images were acquired at different photon energies and the resulting spectra were combined.

SEVI also provides information on the photoelectron angular distribution (PAD). For one-photon detachment, the PAD is given by

$$\frac{d\sigma}{d\Omega} = \frac{\sigma}{4\pi}\left(1 + \beta\left(\frac{3}{2}\cos^2(\theta) - \frac{1}{2}\right)\right)$$

where θ is the angle between the directions of the photoelectron ejection and the polarization of the incident photon.[45] The anisotropy parameter β varies between 2 and −1, and provides information on the angular momentum of the ejected photoelectron and hence on the symmetry of the orbital from which the electron was ejected. Because the value of the anisotropy parameter for a given transition depends on the photon energy, we report PADs as p for $\beta > 0$ and s + d for $\beta < 0$.[46,47]

Electronic structure calculations

Previous computational studies on phenoxy, phenoxide, thiophenoxy, and thiophenoxide suggest that density functional methods can give reasonably accurate results for vibrations and excited electronic states at a modest computational cost.[12,20–25,48] Accordingly, to maintain a consistent level of theory for all species, we calculated the equilibrium geometries and harmonic frequencies for the anions and neutral radicals with the B3LYP hybrid functional[49,50] using the Dunning-style triple-zeta basis set aug-cc-pVTZ.[51] All geometries were restricted to C_{2v} symmetry as shown in Fig. 1, with bond lengths and angles similar to those reported previously.[12,24] All harmonic frequencies were scaled by an empirical factor of 0.9687 to match the level of theory to a test set of experimental vibrational fundamentals.[52] Geometries and relative energies are reported in Table 1 using the atomic numbering scheme shown in Fig. 1; experimental and calculated frequencies are listed in Table 2.

Electronic structure calculations were performed with the Gaussian 09 program.[53] Franck-Condon simulations for the neutral ← anion transitions were carried out with the FCFGAUS09 and PESCAL programs,[54–56] which use the Rosenstock-Chen method to calculate the vibrational wavefunction overlap of harmonic oscillators,[57] with the different normal mode coordinates for the anion and neutral related by Duschinsky rotation.[58,59] Simulations were run with all normal modes, with initial populations given by equal temperature in all vibrations. For each band, the calculated vibrational origin was shifted to match the experimentally

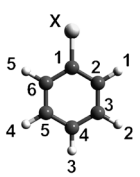

Fig. 1 Structures of the phenoxy and thiophenoxy anions and neutrals in C_{2v} symmetry (X = O, S).

Table 1 Calculated relative energies and equilibrium geometries at the B3LYP/aug-cc-pVTZ level of theory. All energies are in eV, all bond lengths in angstroms, and all angles in degrees. Atom labels refer to Fig. 1, with X = O, S

	C_6H_5O		C_6H_5S		
	Anion	Neutral	Anion	Neutral	
	$^1A_1$	$^2B_1$	$^1A_1$	$^2B_1$	$^2B_2$
E	0.0	2.207	0.0	2.285	2.667
$R(C_1X)$	1.269	1.252	1.744	1.723	1.763
$R(C_1C_2)$	1.443	1.448	1.417	1.414	1.398
$R(C_2C_3)$	1.384	1.372	1.387	1.382	1.389
$R(C_3C_4)$	1.400	1.405	1.396	1.395	1.390
$R(C_2H_1)$	1.085	1.081	1.083	1.081	1.081
$R(C_3H_2)$	1.087	1.082	1.086	1.082	1.082
$R(C_4H_3)$	1.083	1.082	1.083	1.082	1.081
$\theta(C_6C_1C_2)$	113.8	117.1	115.4	118.4	119.6
$\theta(C_1C_2C_3)$	122.6	120.8	122.2	120.6	119.8
$\theta(C_2C_3C_4)$	121.7	120.3	121.1	120.1	120.7
$\theta(C_3C_4C_5)$	117.6	120.7	117.9	120.2	119.3
$\theta(C_1C_2H_1)$	117.0	117.1	117.8	118.6	120.2
$\theta(C_2C_3H_2)$	119.1	120.3	119.2	119.9	119.2

Table 2 Experimental and theoretical frequencies of selected vibrations (in cm^{-1}). Harmonic frequencies are calculated at the B3LYP/aug-cc-pVTZ level of theory and are scaled by an empirical factor of 0.9687

		C_6H_5O		C_6H_5S		
		Anion	Neutral	Anion	Neutral	
	Symm	$^1A_1$	$^2B_1$	$^1A_1$	$^2B_1$	$^2B_2$
Theoretical						
1	a_1	3057	3099	3067	3101	3096
2		3039	3089	3057	3089	3082
3		2996	3068	3018	3070	3066
4		1562	1537	1552	1547	1569
5		1486	1434	1437	1440	1458
6		1356	1375	1149	1162	1169
7		1130	1130	1062	1048	1064
8		990	979	1006	1009	1015
9		956	959	969	977	981
10		797	782	690	709	684
11		517	515	410	414	397
12	a_2	921	963	944	972	956
13		775	783	811	827	822
14		420	369	411	373	408
15	b_1	923	975	944	985	974
16		828	906	847	923	885
17		710	783	715	750	724
18		676	635	682	667	683
19		492	466	471	450	463
20		186	182	160	156	174
21	b_2	3038	3096	3061	3097	3086
22		2999	3074	3023	3079	3072
23		1494	1499	1518	1529	1553
24		1428	1401	1412	1418	1417
25		1300	1298	1297	1303	1313
26		1208	1239	1240	1261	1252
27		1115	1128	1123	1142	1145
28		1035	1057	1041	1062	1063
29		597	578	610	603	610
30		434	433	285	288	237
Experimental						
7						1090(15)
11		505(130)	519(11)	412(18)	427(13)	408(7)

assigned origin, but otherwise the vibrational frequencies and normal mode coordinates were not adjusted to make the simulations match the experiment.

Results

SEVI spectra of phenoxide and thiophenoxide are presented in Fig. 2–4. In all these figures, panel (a) displays the experimental data. The top trace shows a low-resolution overview scan and the lower trace shows a series of high-resolution scans. Panel (b) displays the Franck-Condon simulation, with the transitions convolved by a Gaussian with a FWHM of 15 cm^{-1} to simulate the experimental resolution. The peak positions with errors, PADs, and assignments are summarized in Tables 3 and 4. The low signal-to-noise ratio prevents determination of PADs for some low-intensity transitions. Typical peak widths near threshold are 10–20 cm^{-1}. In general, the resolution of the phenoxide and thiophenoxide spectra is poorer than that of the sulfide calibration spectrum,[44] due to the unresolved rotational structure of the molecular species.

The overview spectra shown in Fig. 2 and 3 exhibit a single progression comprising peaks A–D, with a spacing of 519 cm^{-1} for phenoxide and 427 cm^{-1} for thiophenoxide. For both species, there is a weak transition h below peak A at a similar spacing as the main progression. The overview spectrum of phenoxide is similar to the photoelectron spectrum measured by Gunion *et al.* at a photon energy of 3.408 eV. However, the high-resolution scans reveal that the phenoxide spectrum has a doublet structure that was not seen previously, with the smaller peaks a, b, and c, each lying 51 cm^{-1} lower in energy than peaks A, B, and C. No analogous substructure is observed for thiophenoxide. The higher-energy thiophenoxide spectrum shown in Fig. 4 is dominated by a strong transition E at 21 987 cm^{-1}, with weaker peaks F and G lying 408 cm^{-1} and 1090 cm^{-1} above E. All observed PADs are of s + d character, with values of $-0.1 > \beta > -0.5$ for transitions near threshold.

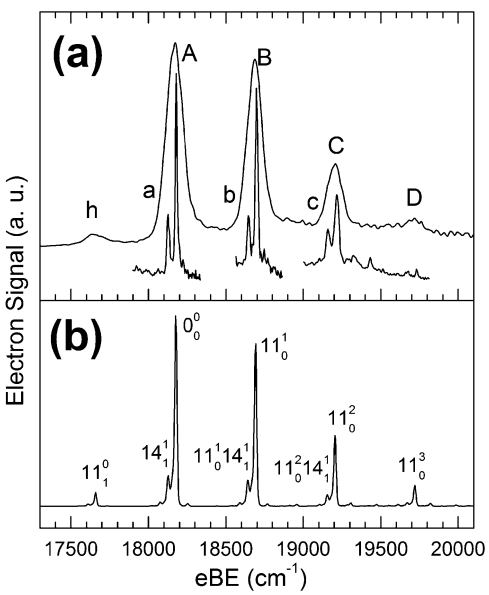

Fig. 2 SEVI spectra of phenoxide covering the $\tilde{X}^2B_1 \leftarrow \tilde{X}^1A_1$ transition compared to simulation. Panel (a) shows a low-resolution overview scan above selected portions of high-resolution scans. Panel (b) shows the FC simulation at 300 K, with a 15 cm^{-1} Gaussian convolution.

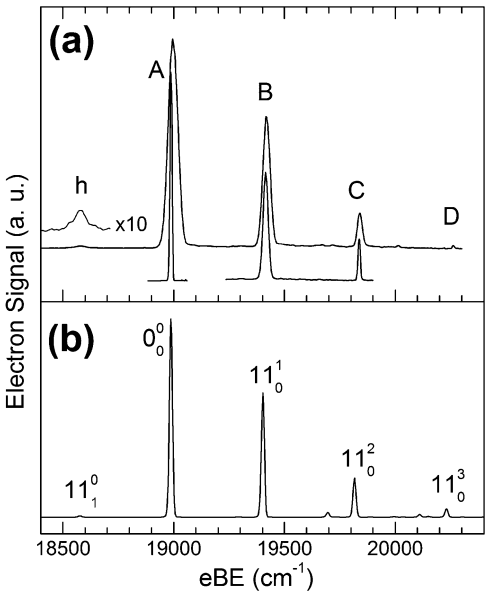

Fig. 3 SEVI spectra of thiophenoxide covering the $\tilde{X}^2B_1 \leftarrow \tilde{X}^1A_1$ transition compared to simulation. Panel (a) shows a low-resolution overview scan above selected portions of high-resolution scans. Peak h is magnified for clarity. Panel (b) shows the FC simulation at 130 K, with a 15 cm^{-1} Gaussian convolution.

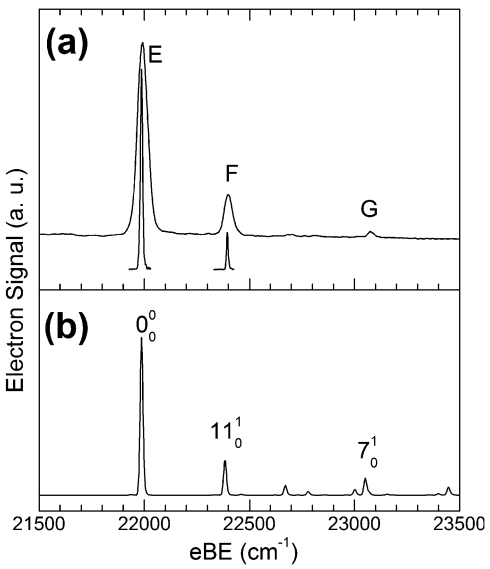

Fig. 4 SEVI spectra of thiophenoxide covering the $\tilde{A}^2B_2 \leftarrow \tilde{X}^1A_1$ transition compared to simulation. Panel (a) shows a low-resolution overview scan above selected portions of high-resolution scans. Panel (b) shows the FC simulation at 130 K, with a 15 cm^{-1} Gaussian convolution.

Analysis and discussion

In this section, we assign the SEVI spectra in detail. The relative energies of the anion and radical species are determined, and vibrational assignments are compared to FC simulations. Results are compared to previous experimental studies. The strong peak A in Fig. 2 and 3 is assigned to the vibrational origin of the $\tilde{X}^2B_1 \leftarrow \tilde{X}^1A_1$ transition for both species, giving electron affinities (EAs) of phenoxy to be 2.2538(8) eV and thiophenoxy to be 2.3542(6) eV. Peak E of the thiophenoxide spectrum is assigned to the origin of the $\tilde{A}^2B_2 \leftarrow \tilde{X}^1A_1$ transition, yielding a term energy of 0.3719(9) eV for the $\tilde{A}^2B_2$ state of thiophenoxy from the splitting between peaks A and E. The PADs are all slightly negative near threshold, indicating nearly s-wave detachment, common for removal of an electron from a localized p orbital or a π bond.[60,61] Since the $\tilde{X}^2B_1$ state is produced by detachment of an electron in a π-bonding orbital, while the $\tilde{A}^2B_2$ state is formed by detachment from a sulfur p orbital, the experimental PADs are consistent with the assigned electronic transitions. The EAs are a further refinement of previous work. Richardson *et al.*[17] used photodetachment spectroscopy to estimate the EA of phenoxy to be ≤2.36(6) eV and thiophenoxy to be ≤2.47(6) eV, while Gunion *et al.*[13] obtained an EA of 2.253(6) eV for phenoxy by anion photoelectron spectroscopy.

In the phenoxide spectrum, peaks A–D are spaced by 519 cm^{-1}. The spacing and intensity distribution of this progression matches the calculated 11_0^n progression in the Franck-Condon simulation. The ν_{11} mode is the lowest-frequency a_1 vibration and its calculated frequency is 515 cm^{-1}. It is an in-plane CCC bend with most of the motion along the $\theta(C_6C_1C_2)$ and $\theta(C_3C_4C_5)$ angles. The change in these angles upon photodetachment (see Table 1) leads to the extended progression in the SEVI spectrum. Similarly, peak h, located 505 cm^{-1} below the origin, is assigned to the 11_1^0 hot band. Although the peak is broad, it matches well with the calculated anion ν_{11} frequency of 517 cm^{-1}.

Peaks a–c appear to be a series of sequence bands trailing the main ν_{11} progression. From the intensity of the 11_1^0 hot band, the vibrational temperature is estimated to be ~300 K,

Table 3 Peak positions, offsets from the origin, PADs, and assignments for the phenoxide SEVI spectra. All energies are in cm^{-1}

Peak	Position	Shift	PAD	Assignment	States
h	17 673(55)	−505		11_1^0	$\tilde{X}^2B_1 \leftarrow \tilde{X}^1A_1$
a	18 127(9)	−51	s + d	14_1^1	
A	18 178(7)	0	s + d	0_0^0	
b	18 646(9)	468	s + d	$11_0^1 14_1^1$	
B	18 697(9)	519	s + d	11_0^1	
c	19 162(14)	984	s + d	$11_0^2 14_1^1$	
C	19 216(14)	1038	s + d	11_0^2	
D	19 712(47)	1534		11_0^3	

Table 4 Peak positions, offsets from the origin, PADs, and assignments for the thiophenoxide SEVI spectra. All energies are in cm^{-1}

Peak	Position	Shift	PAD	Assignment	States
h	18 576(18)	−412		11_1^0	$\tilde{X}^2B_1 \leftarrow \tilde{X}^1A_1$
A	18 988(5)	0	s + d	0_0^0	
B	19 415(12)	427	s + d	11_0^1	
C	19 837(5)	849	s + d	11_0^2	
D	20 262(5)	1274		11_0^3	
E	21 987(5)	0	s + d	0_0^0	$\tilde{A}^2B_2 \leftarrow \tilde{X}^1A_1$
F	22 395(4)	408	s + d	11_0^1	
G	23 077(14)	1090		7_0^1	

so sequence bands as large as those observed should be expected only for modes with frequencies of a few hundred wavenumbers. The intensities and positions of peaks a–c match the simulated $11_0^n14_1^1$ progression in the FC simulation, indicating that the ν_{14} mode is responsible for the sequence bands shown in Fig. 2. This is an a_2 mode, a ring deformation mode with alternating out-of-plane motion for C_2, C_3, C_5, and C_6. Its calculated anion and neutral frequencies are 420 cm^{-1} and 369 cm^{-1}, respectively. The frequency change of −51 cm^{-1} upon photodetachment agrees perfectly with the sequence band positions relative to the main 11_0^n progression. Note that the ν_{14} mode is the second-lowest frequency mode in the anion, according to Table 2. The ν_{20} mode, with b_1 symmetry, has a considerably lower calculated frequency of 186 cm^{-1}, so there is substantial excitation of this mode at the assumed temperature of 300 K. However, its calculated change in frequency upon photodetachment is only −4 cm^{-1}, so the $11_0^n20_1^1$ sequence band is hidden under the envelope of the corresponding 11_0^n peak in the main progression. Other sequence bands involving, for example, the low-frequency ν_{19} and ν_{30} modes contribute to the simulation but are unresolved at our experimental resolution.

The previous phenoxide PE spectrum[13] had insufficient resolution to distinguish between the 11_0^3 transition and a possible 5_0^1 transition, but here we can determine that the ν_5 vibrations are not FC active. Previous experiments had obtained frequencies for the ν_{11} mode of 528 cm^{-1} in aqueous solution[10] and 520 cm^{-1} in a rare-gas matrix,[12] but the only prior gas-phase measurements were from the anion PE spectrum. The ν_{14} sequence bands were also not resolved by Gunion *et al.*, and ν_{14} vibrations have not been observed before for the anion or the neutral $\tilde{X}^2B_1$ state.

The ground state spectrum of thiophenoxide is assigned in much the same way. Peaks A–D are assigned to the 11_0^n progression, with an observed frequency of 427 cm^{-1} compared to 414 cm^{-1} from calculations and 427 cm^{-1} from LIF.[19] Likewise, the weak peak h, 412 cm^{-1} below the origin, is assigned to the ν_{11} hot band, close to the theoretical value of 410 cm^{-1}. This hot band is considerably weaker than the corresponding feature in the phenoxide SEVI spectrum. Its intensity is reproduced in the FC simulations at a lower anion vibrational temperature of ~130 K. At this temperature, only the ν_{20} anion mode has significant excitation, but the 20_1^1 band is calculated to lie only 4 cm^{-1} below the corresponding 11_0^n peak, and is not resolved experimentally. Hence, no sequence band structure is seen in the thiophenoxide SEVI spectrum.

Only two vibrations are observed for the $\tilde{A}^2B_2$ state of thiophenoxy. Peak F, at 408 cm^{-1} above the origin, is assigned to the 11_0^1 transition, since the ν_{11} mode is the only a_1 mode whose calculated frequency, 397 cm^{-1}, is close to the experimental E–F splitting of 408 cm^{-1}. At 1090 cm^{-1} above the origin, peak G best matches the ν_7 fundamental, calculated at 1064 cm^{-1}. The ν_7 mode is a CH bending motion involving the $\theta(C_1C_2H_1)$ and $\theta(C_2C_3H_2)$ angles; the calculated geometries predict a significant change along the $\theta(C_1C_2H_1)$ angle upon photodetachment to the $\tilde{A}^2B_2$ state, consistent with activity in the ν_7 vibration. While Devine *et al.*[25] observed a vibrational structure associated with the $\tilde{A}^2B_2$ state in the photodissociation of thiophenol, their resolution was insufficient to confidently assign the vibrational transitions or obtain definitive values for the vibrational frequencies. The SEVI data represent the first well-characterized experimental values of the vibrations of the $\tilde{A}^2B_2$ state of the thiophenoxy radical.

As stated above, the SEVI spectra directly determine the term energy of the $\tilde{A}^2B_2$ state of thiophenoxy to be 0.3719(9) eV. Our B3LYP calculations predict a splitting of 0.3822 eV, in good agreement with the experimental value. However, the SEVI term energy is higher than the experimental values of 0.32(2) eV and 0.347(5) eV reported from photodissociation experiments of thiophenol by Lim *et al.*[31] and Devine *et al.*,[25] respectively. Previous theoretical values by different methods range from 0.32 eV by MRCI + Q to 0.374 eV by CASPT2, which does not conclusively rule in favor of any of the assignments.[24]

In the work by Lim *et al.*, the photofragment translational energy distribution was determined by ionizing and imaging the H (or D) atom fragment from thiophenol. Features corresponding to the $\tilde{X}^2B_1$ and $\tilde{A}^2B_2$ thiophenoxy states were partially overlapped, making a precise determination of the $\tilde{A}^2B_2$ term energy difficult. The higher resolution experiments by Devine *et al.*, in which the photofragment translational energy distributions were obtained from Rydberg tagging of the H atom, showed a resolved vibrational structure associated with the thiophenoxy $\tilde{X}$ and $\tilde{A}$ states. Interestingly, the separation between the first (*i.e.* lowest internal energy) vibrational peaks seen for the two states was 0.367 eV, which is close to the $\tilde{A}$–$\tilde{X}$ splitting determined from the SEVI spectra. However, based on the pattern of vibrational peaks associated with the $\tilde{A}$ state, they assigned the first resolved peak of the $\tilde{A}$ state to a vibrationally excited feature (with ν_{20} = 1) rather than the vibrational ground state, resulting in the lower $\tilde{A}^2B_2$ term energy reported in their paper. Comparison with the results presented here suggests that the peak in question corresponds to the $\tilde{A}$ state vibrational origin.

Conclusion

Using SEVI, high-resolution photoelectron spectra of phenoxide and thiophenoxide are reported. More accurate values have been determined for the electron affinities of both species, to be 2.2538(8) eV and 2.3542(6) eV, respectively. Several new gas-phase vibrations have been observed. The term energy for the $\tilde{A}^2B_2$ state of thiophenoxy is reported as 0.3719(9) eV, at higher precision but in disagreement with values inferred from photodissociation, suggesting a reassignment of the photodissociation data.

Acknowledgements

This work was supported by the Air Force Office of Scientific Research (AFOSR) under Grant No. FA9550-09-1-0343. We thank Dr Jeong Sik Lim for helpful discussions on the photodissociation of thiophenol. T. I. Y. thanks the National Science and Engineering Research Council of Canada (NSERC) for a doctoral scholarship. The work of C. H. was supported by a Postdoctoral Scholarship of the Deutscher Akademischer Austausch Dienst.

References

1 D. S. Haynes, in *Fossil Fuel Combustion*, ed. W. Bartok and A. F. Sarofim, Wiley, New York, 1991, p. 261.
2 H. Bockhorn, *Soot Formation in Combustion*, Springer-Verlag, New York, 1995.
3 S. Itoh, M. Taki and S. Fukuzumi, *Coord. Chem. Rev.*, 2000, **198**, 3.
4 E. C. Weaver, *Annu. Rev. Plant Physiol.*, 1968, **19**, 283.
5 M. L. Steigerwald, A. P. Alivisatos, J. M. Gibson, T. D. Harris, R. Kortan, A. J. Muller, A. M. Thayer, T. M. Duncan, D. C. Douglass and L. E. Brus, *J. Am. Chem. Soc.*, 1988, **110**, 3046.
6 N. Herron, Y. Wang and H. Eckert, *J. Am. Chem. Soc.*, 1990, **112**, 1322.
7 T. J. Stone and W. A. Waters, *Proc. Chem. Soc.*, 1962, 253.
8 W. T. Dixon and R. O. C. Norman, *J. Chem. Soc.*, 1964, 4850.
9 W. T. Dixon and D. Murphy, *J. Chem. Soc., Faraday Trans. 2*, 1976, **72**, 1221.
10 G. N. R. Tripathi and R. H. Schuler, *J. Chem. Phys.*, 1984, **81**, 113.
11 A. Mukherjee, M. L. Mcglashen and T. G. Spiro, *J. Phys. Chem.*, 1995, **99**, 4912.
12 J. Spanget-Larsen, M. Gil, A. Gorski, D. M. Blake, J. Waluk and J. G. Radziszewski, *J. Am. Chem. Soc.*, 2001, **123**, 11253.
13 R. F. Gunion, M. K. Gilles, M. L. Polak and W. C. Lineberger, *Int. J. Mass Spectrom. Ion Processes*, 1992, **117**, 601.
14 J. G. Radziszewski, M. Gil, A. Gorski, J. Spanget-Larsen, J. Waluk and B. J. Mroz, *J. Chem. Phys.*, 2001, **115**, 9733.
15 G. Porter and F. J. Wright, *Trans. Faraday Soc.*, 1955, **51**, 1469.
16 C. W. Cheng, H. Witek and Y. P. Lee, *J. Chem. Phys.*, 2008, **129**, 154307.
17 J. H. Richardson, L. M. Stephenson and J. I. Brauman, *J. Am. Chem. Soc.*, 1975, **97**, 2967.
18 G. N. R. Tripathi, S. Qun, D. A. Armstrong, D. M. Chipman and R. H. Schuler, *J. Phys. Chem.*, 1992, **96**, 5344.
19 K. Shibuya, M. Nemoto, A. Yanagibori, M. Fukushima and K. Obi, *Chem. Phys.*, 1988, **121**, 237.
20 D. M. Chipman, R. F. Liu, X. F. Zhou and P. Pulay, *J. Chem. Phys.*, 1994, **100**, 5023.
21 Y. Qin and R. A. Wheeler, *J. Chem. Phys.*, 1995, **102**, 1689.
22 H. U. Suter and M. Nonella, *J. Phys. Chem. A*, 1998, **102**, 10128.
23 C. W. Cheng, Y. P. Lee and H. A. Witek, *J. Phys. Chem. A*, 2008, **112**, 2648.
24 C. W. Cheng, Y. P. Lee and H. A. Witek, *J. Phys. Chem. A*, 2008, **112**, 11998.
25 A. L. Devine, M. G. D. Nix, R. N. Dixon and M. N. R. Ashfold, *J. Phys. Chem. A*, 2008, **112**, 9563.
26 I. S. Lim, J. S. Lim, Y. S. Lee and S. K. Kim, *J. Chem. Phys.*, 2007, **126**, 034306.
27 C.-M. Tseng, Y. T. Lee and C.-K. Ni, *J. Chem. Phys.*, 2004, **121**, 2459.
28 M. G. D. Nix, A. L. Devine, B. Cronin, R. N. Dixon and M. N. R. Ashfold, *J. Chem. Phys.*, 2006, **125**, 133318.
29 M. N. R. Ashfold, B. Cronin, A. L. Devine, R. N. Dixon and M. G. D. Nix, *Science*, 2006, **312**, 1637.
30 Z. G. Lan, W. Domcke, V. Vallet, A. L. Sobolewski and S. Mahapatra, *J. Chem. Phys.*, 2005, **122**, 224315.
31 J. S. Lim, I. S. Lim, K. S. Lee, D. S. Ahn, Y. S. Lee and S. K. Kim, *Angew. Chem., Int. Ed.*, 2006, **45**, 6290.
32 A. L. Sobolewski, W. Domcke, C. Dedonder-Lardeux and C. Jouvet, *Phys. Chem. Chem. Phys.*, 2002, **4**, 1093.
33 J. S. Lim, Y. S. Lee and S. K. Kim, *Angew. Chem., Int. Ed.*, 2008, **47**, 1853.
34 J. S. Lim, H. Choi, I. S. Lim, S. B. Park, Y. S. Lee and S. K. Kim, *J. Phys. Chem. A*, 2009, **113**, 10410.
35 D. M. Neumark, *J. Phys. Chem. A*, 2008, **112**, 13287.
36 A. Osterwalder, M. J. Nee, J. Zhou and D. M. Neumark, *J. Chem. Phys.*, 2004, **121**, 6317.
37 A. Eppink and D. H. Parker, *Rev. Sci. Instrum.*, 1997, **68**, 3477.
38 U. Even, J. Jortner, D. Noy, N. Lavie and C. Cossart-Magos, *J. Chem. Phys.*, 2000, **112**, 8068.
39 E. Garand, T. I. Yacovitch and D. M. Neumark, *J. Chem. Phys.*, 2009, **130**, 064304.
40 W. C. Wiley and I. H. McLaren, *Rev. Sci. Instrum.*, 1955, **26**, 1150.
41 D. W. Chandler and P. L. Houston, *J. Chem. Phys.*, 1987, **87**, 1445.
42 E. W. Hansen and P. L. Law, *J. Opt. Soc. Am. A*, 1985, **2**, 510.
43 C. Blondel, W. Chaibi, C. Delsart and C. Drag, *J. Phys. B: At., Mol. Opt. Phys.*, 2006, **39**, 1409.
44 E. Garand and D. M. Neumark, *J. Chem. Phys.*, 2011, **135**, 024302.
45 K. L. Reid, *Annu. Rev. Phys. Chem.*, 2003, **54**, 397.
46 J. Cooper and R. N. Zare, *J. Chem. Phys.*, 1968, **48**, 942.
47 C. Bartels, C. Hock, J. Huwer, R. Kuhnen, J. Schwobel and B. von Issendorff, *Science*, 2009, **323**, 1323.
48 W. G. Xu and A. F. Gao, *J. Phys. Chem. A*, 2006, **110**, 997.
49 A. D. Becke, *J. Chem. Phys.*, 1993, **98**, 5648.
50 C. T. Lee, W. T. Yang and R. G. Parr, *Phys. Rev. B: Condens. Matter*, 1988, **37**, 785.
51 T. H. Dunning, *J. Chem. Phys.*, 1989, **90**, 1007.
52 J. P. Merrick, D. Moran and L. Radom, *J. Phys. Chem. A*, 2007, **111**, 11683.
53 M. J. Frisch, G. W. Trucks, H. B. Schlegel, G. E. Scuseria, M. A. Robb, J. R. Cheeseman, G. Scalmani, V. Barone, B. Mennucci, G. A. Petersson, H. Nakatsuji, M. Caricato, X. Li, H. P. Hratchian, A. F. Izmaylov, J. Bloino, G. Zheng, J. L. Sonnenberg, M. Hada, M. Ehara, K. Toyota, R. Fukuda, J. Hasegawa, M. Ishida, T. Nakajima, Y. Honda, O. Kitao, H. Nakai, T. Vreven, J. A. Montgomery, Jr, J. E. Peralta, F. Ogliaro, M. Bearpark, J. J. Heyd, E. Brothers, K. N. Kudin, V. N. Staroverov, T. Keith, R. Kobayashi, J. Normand, K. Raghavachari, A. Rendell, J. C. Burant, S. S. Iyengar, J. Tomasi, M. Cossi, N. Rega, J. M. Millam, M. Klene, J. E. Knox, J. B. Cross, V. Bakken, C. Adamo, J. Jaramillo, R. Gomperts, R. E. Stratmann, O. Yazyev, A. J. Austin, R. Cammi, C. Pomelli, J. W. Ochterski, R. L. Martin, K. Morokuma, V. G. Zakrzewski, G. A. Voth, P. Salvador, J. J. Dannenberg, S. Dapprich, A. D. Daniels, O. Farkas, J. B. Foresman, J. V. Ortiz, J. Cioslowski and D. J. Fox, *Gaussian 09, Revision B.01*, Gaussian, Inc., Wallington, CT, 2010.
54 K. M. Ervin, *FCFGAUS09a*, 2010.
55 K. M. Ervin, *PESCAL, Fortran Program*, 2010.
56 K. M. Ervin, T. M. Ramond, G. E. Davico, R. L. Schwartz, S. M. Casey and W. C. Lineberger, *J. Phys. Chem. A*, 2001, **105**, 10822.
57 P. Chen, in *Unimolecular and Bimolecular Reaction Dynamics*, ed. T. Baer, C.-Y. Ng and I. Powis, John Wiley & Sons, Chichester, 1994, p. 371.
58 F. Duschinsky, *Acta Physicochim. URSS*, 1937, **7**, 551.
59 T. I. Yacovitch, E. Garand and D. M. Neumark, *J. Chem. Phys.*, 2009, **130**, 244309.
60 K. J. Reed, A. H. Zimmerman, H. C. Anderson and J. I. Brauman, *J. Chem. Phys.*, 1976, **64**, 1368.
61 M. J. Nee, A. Osterwalder, J. Zhou and D. M. Neumark, *J. Chem. Phys.*, 2006, **125**, 014306.